Life Sciences 227 (2019) 82–93

Contents lists available at ScienceDirect

Life Sciences

journal homepage: www.elsevier.com/locate/lifescie

Astragaloside IV exerts angiogenesis and cardioprotection after myocardial infarction via regulating PTEN/PI3K/Akt signaling pathway

Songyi Cheng[a], Xiaoxiao Zhang[b], Qian Feng[b], Jiandong Chen[c], Le Shen[c], Peng Yu[c], Li Yang[d], Daohai Chen[e], Haowen Zhang[b], Weixin Sun[b], Xiaohu Chen[c,*]

[a] Nanjing Hospital of Chinese Medicine, Affiliated to Nanjing University of Chinese Medicine, Nanjing, China
[b] Nanjing University of Chinese Medicine, Nanjing, China
[c] Jiangsu Province Hospital of Traditional Chinese Medicine, Affiliated Hospital of Nanjing University of Chinese Medicine, Nanjing, China
[d] Daguang Road Community Health Service Center of Qinhuai District, Nanjing, China
[e] Changzhou Hospital of Traditional Chinese Medicine, Changzhou, China

ARTICLE INFO

Keywords:
Astragaloside IV
Acute myocardial infarction
Angiogenesis
PTEN/PI3K/Akt signaling pathway

ABSTRACT

Aims and methods: Acute myocardial infarction (AMI) is a common cardiovascular disease with high mortality. Astragaloside IV (AS-IV) was reported to have cardioprotective effect after AMI. We hypothesize that the cardioprotective role of AS-IV is exerted by enhancing angiogenesis via regulating PTEN/PI3K/Akt signaling pathway. To valid our hypothesis, AMI rats and human umbilical vein endothelial cells (HUVECs) were employed in our study.

Key findings: After treatment, cardiac function, survival rate, infarct size, pathological changes and fibrosis, cell apoptosis, ultrastructural changes, angiogenesis and expression of PTEN/PI3K/Akt signaling pathway were evaluated, respectively. In vitro study we detected proliferation, tube formation and signaling pathway activation of HUVECs treated with AS-IV, lentivirus overexpressed PTEN was employed to elucidate the potential mechanism. The results indicated that AS-IV administration significantly improved cardiac function and survival rate, limited infarct size, ameliorated pathological changes and fibrosis deposition, inhibited apoptosis, relieved ultrastructure injury and enhanced angiogenesis, PTEN/PI3K/Akt signaling pathway was activated simultaneously compared to the model group. In vitro study suggested that AS-IV treatment promoted cell proliferation and tube formation, and induced PTEN/PI3K/Akt signaling pathway activation. Importantly, overexpression of PTEN by lentivirus abolished AS-IV-induced angiogenesis.

Significance: Our study indicated that AS-IV could promote angiogenesis and cardioprotection after myocardial infarction. The mechanisms involve activation of PTEN/PI3K/Akt signaling pathway.

1. Introduction

Coronary artery disease, which is also called ischemic heart disease, has become a major cause of morbidity and mortality worldwide and brings about social economic burden [1]. As the most severe subtype, acute myocardial infarction (AMI) often leads to sudden death. People who survived from the acute phase may also suffer from subsequent complications such as angina pectoris and heart failure [2]. Currently the mainstream therapeutic strategy for coronary artery disease is revascularization of the accused vessels as early as possible, such as percutaneous coronary intervention (PCI) or coronary artery bypass grafting (CABG). However, the overall effectiveness is limited [3]. Meanwhile, many conditions are not available for conventional revascularization techniques such as patients with coronary artery diffuse stenosis [4] or iodinated contrast media hypersensitivity [5], etc. Therefore, a novel medical treatment which promotes reperfusion of ischemic myocardium is needed.

Angiogenesis refers to the generation of newly formed vascular from pre-existing capillaries [6]. Promoting reperfusion and systolic/diastolic function of the ischemic myocardium through therapeutic angiogenesis appeared a promising strategy [7]. For decades, researchers were dedicated to find out an optimal way to enhance the angiogenesis effect in pathologic status. Up to now, delivery of growth factors through different approaches is the most common method, such as vascular endothelial growth factor (VEGF) [8] and fibroblast growth factors (FGFs) [9]. However, the results of these strategies are not that

* Corresponding author at: Jiangsu Province Hospital of Traditional Chinese Medicine, Department of Cardiology, Hanzhong Road 155#, Nanjing 210029, Jiangsu, China.
E-mail address: chenxhdoctor@sina.com (X. Chen).

https://doi.org/10.1016/j.lfs.2019.04.040
Received 12 February 2019; Received in revised form 8 April 2019; Accepted 16 April 2019
Available online 17 April 2019

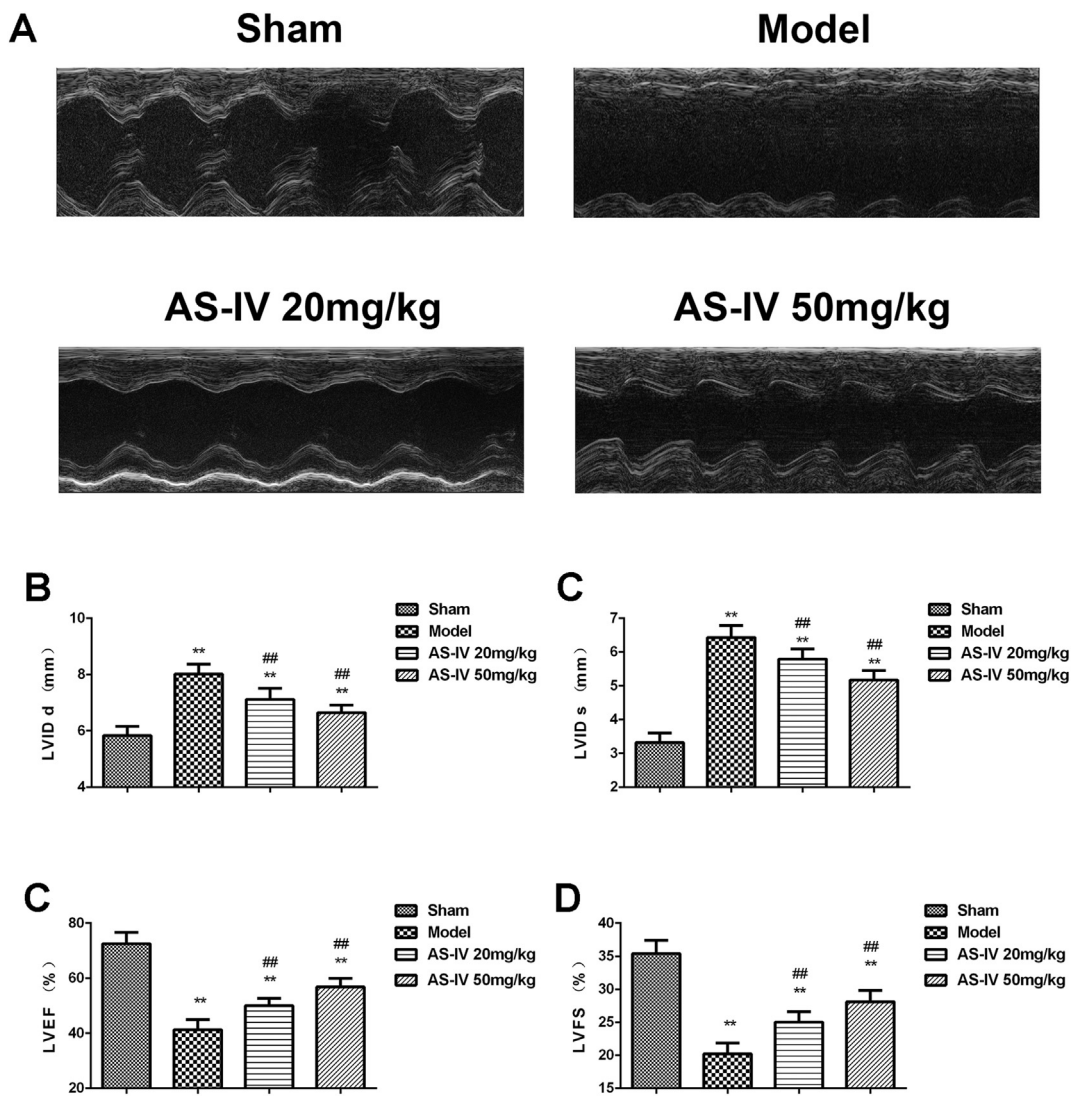

Fig. 1. Echocardiography evaluation of cardiac function. (A) Representative M-mode echocardiographic images from sham, model, low-dose and high-dose of AS-IV groups recorded after treatment. (B) LVIDs of each group recorded after 14 days treatment. (C) LVIDd of each group recorded after 14 days treatment. (D) LVEF of each group recorded after 14 days treatment. (E) LVFS of each group recorded after 14 days treatment. n = 10 rats per group. $^{**}P < 0.01$ compared with the sham group. $^{\#\#}P < 0.01$ compared with the model group.

desirable for various reasons [10]. On the contrary, excessive exogenous growth factors might increase the risk of oncogenesis and metastasis.

Astragaloside IV (AS-IV) is a major monomer extracted from Astragalus membranaceus, a classic Chinese herbal medicine which has been used for over 2000 years [11]. Previous studies suggested that Astragaloside IV has diverse pharmacological activities, such as antioxidative stress [12], suppressing inflammation [13], inhibiting apoptosis [14] and stimulating energy metabolism [15], etc. Astragaloside IV was also widely used in treating cardiovascular diseases with distinct pharmacological action [16–18]. Whether AS-IV is capable of ameliorating AMI through enhancing angiogenesis arouses our interest. In the present study, rat model of AMI and human umbilical vein endothelial cells (HUVECs) were employed to valid our hypothesis, and we further explored the mechanism through PTEN/PI3K/Akt signaling pathway, a key signaling pathway involved in angiogenesis, in order to provide new targets for further research.

2. Material and methods

2.1. Animals and reagents

60 male Sprague–Dawley rats (300 ± 20 g, 10–12 weeks) provided by the Comparative Medicine Centre of Yangzhou University (Yangzhou, China) were employed in this study. Every four of the rats were raised in sterilized cages and received a 12 h light/dark cycle in accordance with the guidelines of the Animal Care and Use Committee of the Nanjing University of Chinese Medicine. The experimental was conducted following the Ethics Review of Lab Animal Use Application of Nanjing University of Chinese Medicine. AS-IV was purchased from National Institute for the Control of Pharmaceutical and Biological Products (Beijing, China).

2.2. Establishment of AMI and grouping

Anesthesia was performed by intraperitoneal injection of pentobarbital sodium (50 mg/kg, Sigma-Aldrich, St. Louis, USA) before surgery. A ventilator (HX-300S; Chengdu Techman software Co., Ltd. Chengdu, China) was connected through tracheal intubation to

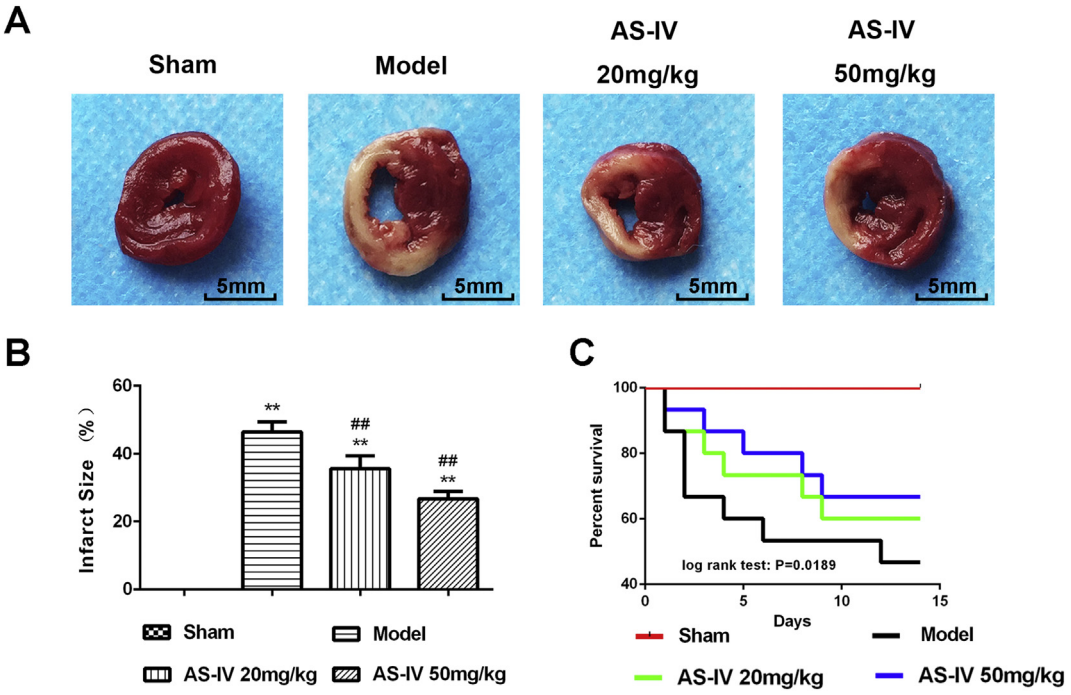

Fig. 2. Representative images of TTC staining. (A) AS-IV limited myocardial infarct size after AMI. The infarcted area (white) and the normal myocardium (red) from each section were measured by Image J. (B) Ratios of infarcted area vs. left ventricular area (RA/LV) are presented in the graph. n = 6 rats per group. (C) Survival rate after treatment for 2 weeks. n = 15 rats per group. Log rank test: P = 0.0189. **P < 0.01 compared with the sham group. ##P < 0.01 compared with the model group. (For interpretation of the references to color in this figure legend, the reader is referred to the web version of this article.)

maintain normal respiration with rate of 60 breaths per minute and tidal volume of 1.5–2 mL. Then the thoracic cavity was exposed through a left thoracotomy. Left anterior descending coronary artery (LAD) was ligated by a 6-0 silk suture between pulmonary and left auricle. The validation of successful AMI model depended on the color change of left ventricle anterior part. Rats in the sham group didn't receive LAD ligation, instead, silk suture just passed through the myocardium. After the procedure closed thoracic cavity with 4–0 silk suture. Intramuscular injection of 2×10^4 U penicillin (Lukang, Shandong, China) was performed following the operation. Rats survived from the surgery were allocated as 4 groups: sham operated group (n = 15), AMI group (n = 15), AS-IV low-dose group (20 mg/kg/d, n = 15) and AS-IV high-dose group (50 mg/kg/d, n = 15); AS-IV was intragastric administrated for 2 weeks; equal normal saline were intragastric administrated every day in AMI group and sham operated group.

2.3. Measurement of echocardiography

Cardiac function and structure were assessed via high-frequency ultrasound system Vevo2100 (VisualSonics Inc., Toronto, ON, Canada). Briefly, rats were anesthetized with isoflurane (5%) using a ventilation equipment, carefully removed fur on the left chest, then two-dimensional echocardiographic measurements were obtained. Left ventricular internal diastolic and systolic diameter (LVIDd and LVIDs), together with the left ventricular ejection fraction and fractional shortening (LVEF and LVFS) were measured from M-mode tracing.

2.4. Detection of myocardial infarction size

After the rats were sacrificed, hearts were harvested immediately and stored at −20 °C for approximately 20 mins in order to harden tissue. Then, the hearts were cut into 2 mm slices, incubated with 2% tetrazolium chloride (TTC, Sigma-Aldrich, St. Louis, USA) at 37 °C for about 30 min and then fixed in 10% neutral formalin. Infarct sites were pale white, while normal tissues were dark red. Slices of heart were photographed and the area of infarct was calculated with Image J (NIH, Bethesda, USA).

2.5. Test of histopathology

Rats' hearts were fixed in 10% neutral formalin overnight and embedded in paraffin (Kemiou Chemical Reagent Co.). Then cut the hearts into 4-μm-thick sections, followed by hematoxylin and eosin (HE) and Masson's trichrome staining. The histopathology change and fibrosis with/without treatment were evaluated. Each section was imaged by a microscopy (DP73; Olympus, Tokyo, Japan). Fibrosis area vs. normal area was calculated by Image J (NIH, Bethesda, USA).

2.6. Assessment of ultrastructural injury

Rats' hearts were obtained and sliced into cubes for 1 mm^3 then fixed in 4% glutaraldehyde and 4% osmium tetroxide for 24 h successively. The samples were dehydration with acetone, embedded in paraffin resin and cut into sections by a microtome (Reichert UltracutE, Leica, USA). Next the samples were stained with 1% uranyl acetate and 0.2% lead citrate. Images were captured by transmission electron microscopy TEM (JEM-1010; Olympus Corporation) at 25000×.

2.7. Measurement of apoptosis by TUNEL/DAPI immunofluorescence

Cell apoptosis after treatment in each group was evaluated by TUNEL staining fluorescence detection kit (Beyotime Institute of Biotechnology). DAPI (Sigma, St Louis, USA) staining was employed to assess the number of nucleus. TUNEL-positive cells were observed under a fluorescent microscope (Leica, Buffalo Grove, USA) at 400 × magnification. Image J (NIH, Bethesda, MD) was used to determine the area of TUNEL and DAPI-positive staining.

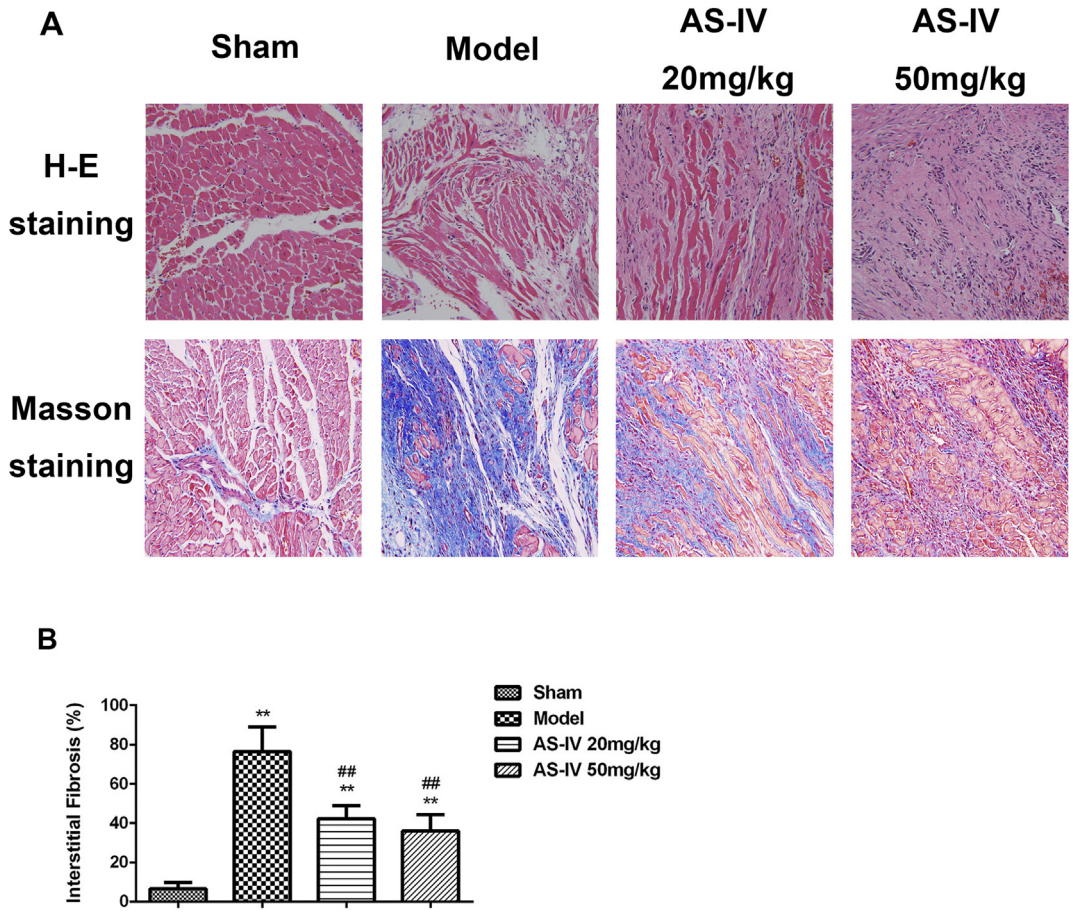

Fig. 3. Assessment of H-E and Masson's staining (400× magnification). (A) H-E and Masson's trichrome staining of infarcted rat myocardium in different groups. In the Masson's trichrome stained sections, blue represents the fibrous tissue. (B) Ratios of fibrosis tissue vs. normal tissue. **P < 0.01 compared with the sham group. ##P < 0.01 compared with the model group. (For interpretation of the references to color in this figure legend, the reader is referred to the web version of this article.)

2.8. Evaluation of microvessel density

α-SMA is expressed in newly formed vascular endothelial cells, hence immunohistochemical technique was used to evaluate angiogenesis after treatment. According to the method described in previously study, the positive signal of α-SMA in the newly formed vascular was stained with orange-yellow. The microvessels were counted under a microscope (DP73; Olympus, Tokyo, Japan) at a magnification of ×400. Percentage of angiogenesis was calculated and averaged by Image J (NIH, Bethesda, USA).

2.9. Cell culture and treatment

HUVECs were provided by American Type Culture Collection (ATCC, Rockville, MD). The cells were cultured in endothelial growth medium (Gibco, MA, USA) at 37 °C in 5% CO_2. The medium was substituted every 2 days. Cells were treated with different concentration of AS-IV (10–160 μmol/L).

2.10. Lentivirus transfection

Lentivirus to overexpress PTEN and blank lentivirus (GFP) were designed and constructed by GeneChem (Shanghai, China).Cells were pre-cultured in 24-well plates (1×10^5/well) for 24 h and then treated with 5 μg/mL Polybrene (Sigma-Aldrich, Shanghai, China) and lentivirus suspension, and cultured for 72 h. Then the medium was replaced by fresh medium, and BD FACSCanto (BD Biosciences, San Jose, CA) was used to detect the transfection efficiency after 72 h.

2.11. Cell proliferation assay

CCK-8 assay (Beyotime Biotechnology, Haimen, Jiangsu, China) was purchased and employed to evaluate HUVECs viability according to the protocol. HUVECs were inoculated in 96-well plates at a density of 2×10^4 cell/well for 24 h, then exposed to 10 μL CCK-8 reagents under different treatments and incubated at 37 °C for additional 4 h. Absorbance values at the wavelength of 450 nm were detected after incubation on an automated plate reader (Tecan Group Ltd., Mannedorf, Switzerland).

2.12. Tube formation assay

Matrigel angiogenesis assay was performed as previously described [19]. Cells (8×10^4 cells/well) under different treatments were dispensed onto the Matrigel (BD Bioscience, San Jose, CA, USA). Then the cells were incubated at 37 °C for 18 h. The tube formation was analyzed by taking four 100× images of each well and calculating the number of nodes and total tube length.

2.13. Western blotting analysis

Total protein was isolated from the left ventricular tissue and HUVECs according to the standard protocols. Subsequently the protein concentration was determined by BCA assay (Roche, USA). The separated proteins were then transferred onto polyvinylidene fluoride (PVDF; Millipore, Billerica, USA) membranes with transfer box (Bio-Rad Laboratories, Hercules, USA). The resulting membranes were

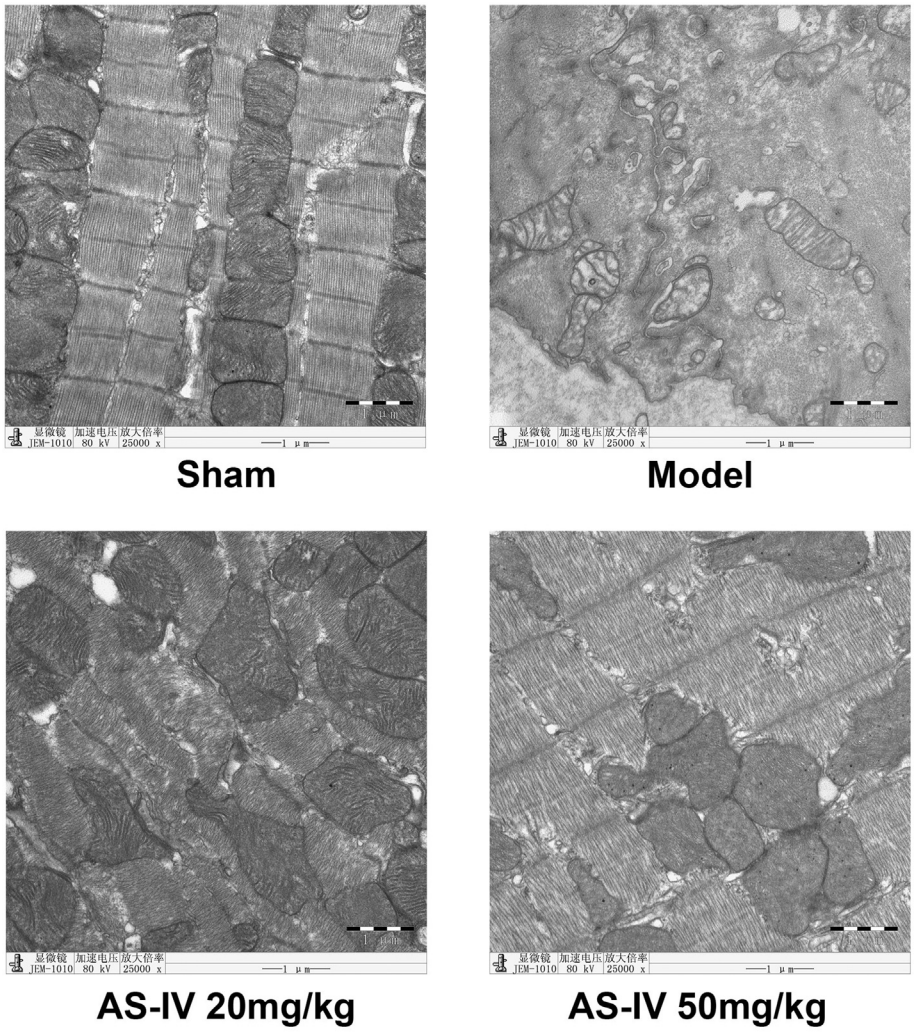

Fig. 4. Representative images of TEM from different groups at 25000 × magnification. In sham group, the myofilaments were neatly arranged, shape and size of mitochondria were normal. The structure of the myofilaments was seriously damaged in model group, and the swollen mitochondria could be found. Rats received AS-IV treatment exhibited less injured mitochondria, and the structure of the myofilaments was improved compared to model group.

blocked with 5% bovine serum albumin (BSA, Beyotime Institute of Biotechnology) for 1 h at room temperature and then incubated with corresponding primary antibodies obtained from Abcam (Cambridge, MA, USA) including rabbit anti-Bax (1:1000), rabbit anti-Bcl-2(1:1000), rabbit anti-PTEN(1:1500), rabbit anti-PI3K (1:2000), rabbit anti-VEGF (1:1000), rabbit anti-p-AKT(1:1000), anti-AKT(1:1000) and rabbit anti-β-actin (1:800) overnight at 4 °C. After carefully washing with Tris-buffered saline with tween (TBST), the membrane was incubated with HRP-conjugated secondary antibodies (1:2000) at room temperature for 1 h. The protein band was detected and captured by a chemiluminescence image analyzer (GE Healthcare, Uppsala, Sweden). The mean gray values of the bands were analyzed by Image J (NIH, Bethesda, USA).

2.14. Statistical analysis

SPSS 22.0 and GraphPad Prism 5 software were employed for statistical processing and graph making. Each experiment was repeated in triplicate. Values are expressed as mean ± standard error. One-way ANOVA and Tukey test was performed to evaluate the statistical parameters between the groups and determine post hoc differences. Kaplan-Meier survival analysis was employed to calculate survival rates of the rats after treatment. P-value < 0.05 was considered as statistically significant.

3. Results

3.1. AS-IV administration significantly improved cardiac function after AMI

We evaluated the effect of AS-IV on cardiac function after AMI. Fig. 1A shows representative M-mode echocardiographic images from sham-operated group, model group and different dosages-treated groups recorded 14 days after AMI. Fig. 1B and C show that LVIDd and LVIDs were remarkably reduced after 14 days AS-IV treatment, compared to model group. EF and FS values in AS-IV-treated groups were also significantly improved (Fig. 1D and E). The rats in the high-dose AS-IV group (50 mg/kg) appeared to have a better recovery of cardiac function.

3.2. AS-IV administration significantly improved survival rate and limited infarcted size after AMI

Kaplan-Meier survival analysis and TTC staining were employed to evaluate the effect of the AS-IV after AMI. Fig. 2A shows that hearts harvested from different groups. Red region represented for survived myocardium while pale region referred to necrotic tissue. Fig. 2B demonstrated that the infarct size of rat hearts. Fig. 2C reveals that the survival rate of the rats. AS-IV treatment significantly improved survival rate and decreased infarct size compared with rats in model group

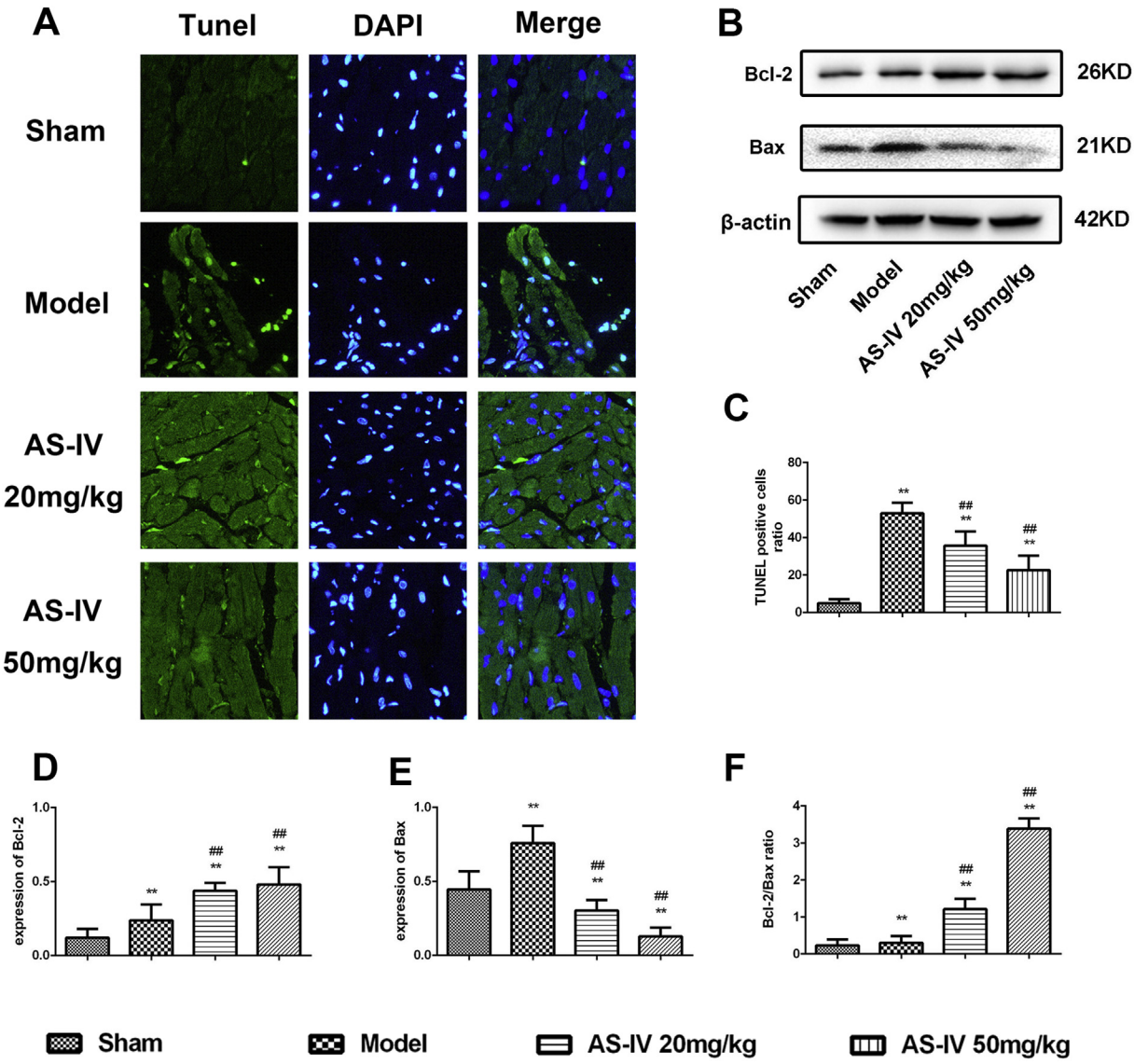

Fig. 5. Evaluation of myocardium apoptosis. (A) Representative images of TUNEL/DAPI immunofluorescence (400× magnification). Green fluorescence represents apoptosis cells, while blue fluorescence refers to DAPI-positive cells. (B) Level of Bcl-2 and Bax in rats from different groups measured by western blotting. (C) Ratios of TUNEL-positive cells vs. DAPI-positive cells. Quantified analysis of Bcl-2 (D), Bax (E), and the Bcl-2/Bax ratio (F).β-actin served as the internal control.**P < 0.01 compared with the sham group. ##P < 0.01 compared with the model group. (For interpretation of the references to color in this figure legend, the reader is referred to the web version of this article.)

(Fig. 2B, C). Rats in high-dose group had better survival condition and smaller infarcted size than that in low-dose group, indicated that the protection was dose-dependent.

3.3. Pathological changes and fibrosis in myocardium were ameliorated after AS-IV administration

Ischemia not only causes dysfunction of myocardial cells, but also results in cell morphological changes. H-E staining was used in this study to assess cardio-protection of AS-IV in terms of Pathological changes. As shown in Fig. 3A, myocardial cells in model group had critical damage, necrotic tissue was infiltrated by numerous neutrophils. Survived myocardial cells presented derangement distribution compared to the sham group. Nevertheless, rats in AS-IV treated groups exhibited significant amelioration. Masson's trichrome staining was performed to detect fibrosis deposition in myocardium. Fibrous tissue stained blue and myocardial fibers stained red. Collagen content and disarray of myocardial fibers was significantly increased in the model group compared with the sham group. Ratios of fibrosis tissue vs. normal tissue are presented in Fig. 3B. However, AS-IV treatment with different doses ameliorated myocardial fibrosis to varying degrees, the collagen content was remarkably decreased compared with model group, and high-dose treatment achieved better therapeutic efficacy.

3.4. AS-IV administration significantly alleviated myocardium ultrastructural impairment after AMI

Myocardial tissue was observed under TEM to evaluate the ultrastructure of myocardium (Fig. 4). Cardiomyocytes in sham group showed a regular distribution of mitochondria and glycogen between sarcomeric units, normal mitochondria were linearly arranged without crista defects, swelling or vacuolation. In contrast, cardiomyocyte in model group was seriously injured, with most mitochondria having a swollen matrix and cristae that were shortened and shrunken. Glycogen deposits were present between myofibrils in some regions. Treatment of AS-IV maintained integrity of sarcolemma and fascicle, the structure of

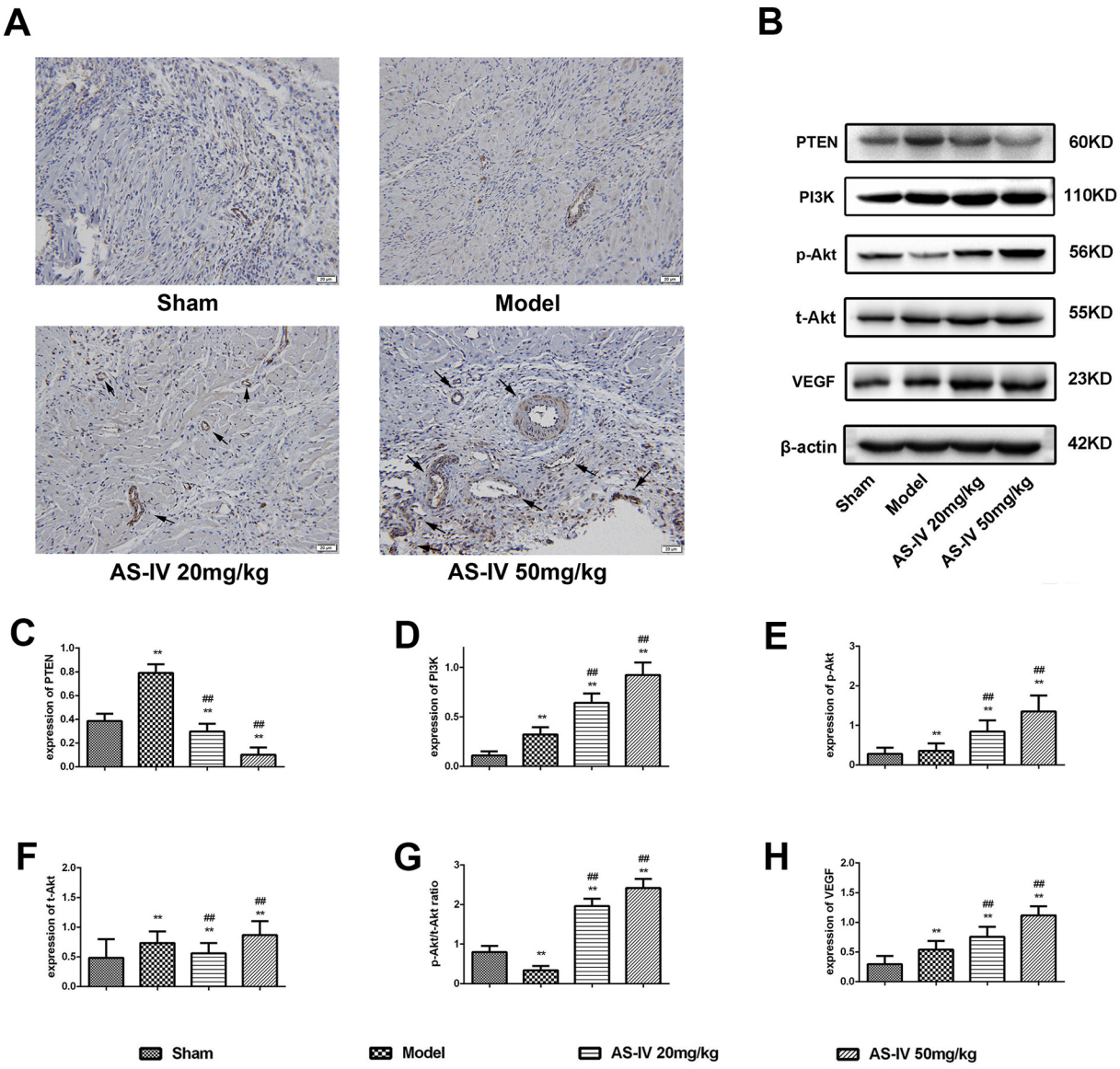

Fig. 6. Assessment of angiogenesis and signaling pathway activation after treatment. (A) Representative images of immunohistochemical analysis at 400× magnification. Orange spots (arrows) indicate α-SMA positive cells, which also represent newly formed vessels. (B) Expression of PTEN/PI3K/Akt signaling pathway and VEGF from different groups measured by western blotting. Quantified western blot results of PTEN(C), PI3K (D), p-Akt (E), t-Akt(F), p-Akt/p-Akt ratio (G) and VEGF (H)are provided.β-actin served as the internal control.**P < 0.01 compared with the sham group. ##P < 0.01 compared with the model group. α-SMA, alpha smooth muscle actin.

mitochondria were also remained, swelling and vacuolar degeneration could be hardly seen. The improvement was more notable in high-dose group compared with low dose-group.

3.5. AS-IV administration significantly relieved ischemic-induced myocardial apoptosis

Myocardium apoptosis and expression of Bcl-2/Bax were evaluated by TUNEL assay and Western blotting assay 14 days after ligation procedures, respectively (Fig. 5). Due to ischemia, there was more apoptosis myocardium in model group than those in sham group. Similarly, the apoptosis rate in model group was significantly higher compared with sham group. Western blotting indicated that pro-apoptosis factor (Bax) was downregulated and anti-apoptosis factor (Bcl-2) was upregulated compared with sham group. In the groups performed AS-IV therapy, myocardium apoptosis and apoptosis rate were significantly reduced, related proteins expression were altered as well. Anti-apoptosis effect was more remarkable in high-dose AS-IV treated group than that in low-dose AS-IV treated group.

3.6. AS-IV administration promoted angiogenesis and activated the PTEN/PI3K/Akt signaling pathway after AMI

We evaluated the microvascular formation after AMI in different groups by using immunohistochemistry with the antibody for α-SMA. It is also reported that PTEN/PI3K/Akt signaling pathway was crucially involved in new vascular formation process. Thus, we examined the expression of proteins in PTEN/PI3K/Akt signaling pathway. As shown in Fig. 6A, at the border zone of infarcted myocardium, newly formed capillaries was stained orange. Compared with sham group, slightly increase of newly formed capillaries in model group was observed 2 weeks after operation. Newly formed capillaries density was significantly increased in both high and low dose AS-IV treated rats compared to that of the model group and sham operated group. In the high dose AS-IV treated group, newly formed capillaries density was higher than that in low dose group. Fig. 6B revealed that PTEN

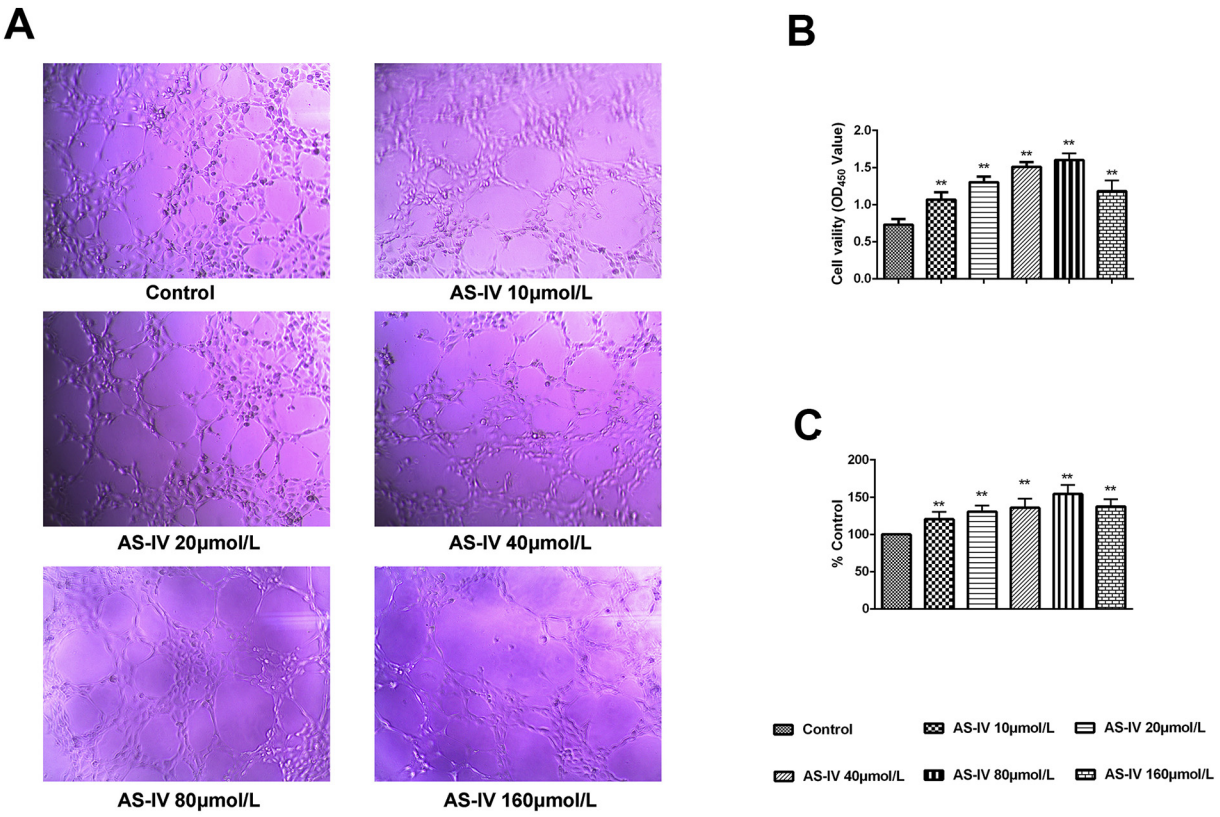

Fig. 7. Evaluation of cell proliferation and tube formation. (A) Representative images of Matrigel tube formation assay analysis at 200× magnification. Cells were incubated with different dosage (10 μmol/L to 160 μmol/L) of AS-IV for 18 h. (B) Proliferation of HUVECs treated with different dosage (10 μmol/L to 160 μmol/L) of AS-IV was detected by CCK-8 assay. (C) Bar graph of tube formation assessment with different dose of AS-IV, data were analyzed as tube percentage versus control group. **P < 0.01 compared with the control group. AS-IV, astragaloside IV; CCK-8, Cell Counting kit 8.

expression was upregulated in model group compared with sham operated group, while AS-IV treatment induced significant suppression of PTEN level in a dose-depended manner. Expression of PI3K was decreased in model group compared with sham group, and increased in AS-IV treated groups in a dose-depended manner compared with sham group. There was no difference between sham group and model group in terms of Akt phosphorylation, and Akt phosphorylation was enhanced in AS-IV treated groups in a dose-depended manner. Total Akt level changes were not observed in all groups. Expression changes of VEGF were similar to PI3K and Akt phosphorylation. This implicated that AS-IV could upregulate expression of VEGF and PTEN/PI3K/Akt pathway might be involved in AS-IV induced angiogenic action in AMI rats.

3.7. AS-IV augmented proliferation and tube formation in HUVECs

To explore the roles of pro-angiogenesis effect induced by AS-IV, we investigated cell proliferation and tube formation in AS-IV-treated HUVECs using CCK-8 and Matrigel tube formation assays, respectively. HUVECs were incubated with different concentration of AS-IV (10-160 μmol/L). As shown in Fig. 7B, AS-IV exposure induced significant upregulation of cell proliferation with a dose-dependent manner from 10 μmol/L to 80 μmol/L, when the concentration reached 160 μmol/L, cell proliferation began to decrease. AS-IV also enhanced cell tube formation. At the concentration of 80 μmol/L AS-IV gained optimal effect. (Fig. 7A and C).

3.8. AS-IV activated the PTEN/PI3K/Akt signaling pathway in HUVECs

In vivo study we observed activated PTEN/PI3K/Akt signaling pathway and upregulated VEGF expression. In this section, HUVECs were cultivated with AS-IV (10–160 μmol/L) to explore the optimal concentration in vitro. We examined PTEN, PI3K, VEGF and Akt phosphorylation, the results indicated that AS-IV suppressed expression of PTEN and increased the levels of PI3K, VEGF and phosphorylated Akt in a dose-dependent manner and 80 μmol/L is the optimal concentration for activating PTEN/PI3K/Akt signaling pathway. (Fig. 8).

3.9. AS-IV promoted angiogenesis via downregulating PTEN expression

Lentivirus overexpressed PTEN was constructed and transfected to HUVECs in order to clarify whether AS-IV was involved in enhancing angiogenesis followed by activating PTEN/PI3K/Akt signaling pathway through downregulating PTEN expression. Results demonstrated that co-treatment of lentivirus overexpressed PTEN significantly decreased AS-IV induced cell proliferation compared with AS-IV (80 μmol/L) treated HUVECs. Matrigel assay indicated that tube formation induced by AS-IV was also diminished due to overexpressing PTEN. Lastly, Western Blotting assay suggested that exogenously overexpressed PTEN could abrogate upregulated expression of PI3K, VEGF and Akt phosphorylation induced by AS-IV. All those above indicated that inhibition of PTEN by AS-IV activated downstream of PTEN/PI3K/Akt signaling pathway and then promoted angiogenesis (Fig. 9).

4. Discussion

The major finding in this study is that administration of AS-IV elicited a significant cardioprotection in improving cardiac function and survival rate, limiting infarct size, ameliorating myocardial fibrosis and remodeling, inhibiting apoptosis, alleviating ultrastructural impairment, and promoting angiogenesis after permanent LAD ligation. Activation of angiogenesis associated signaling pathway PTEN/PI3K/

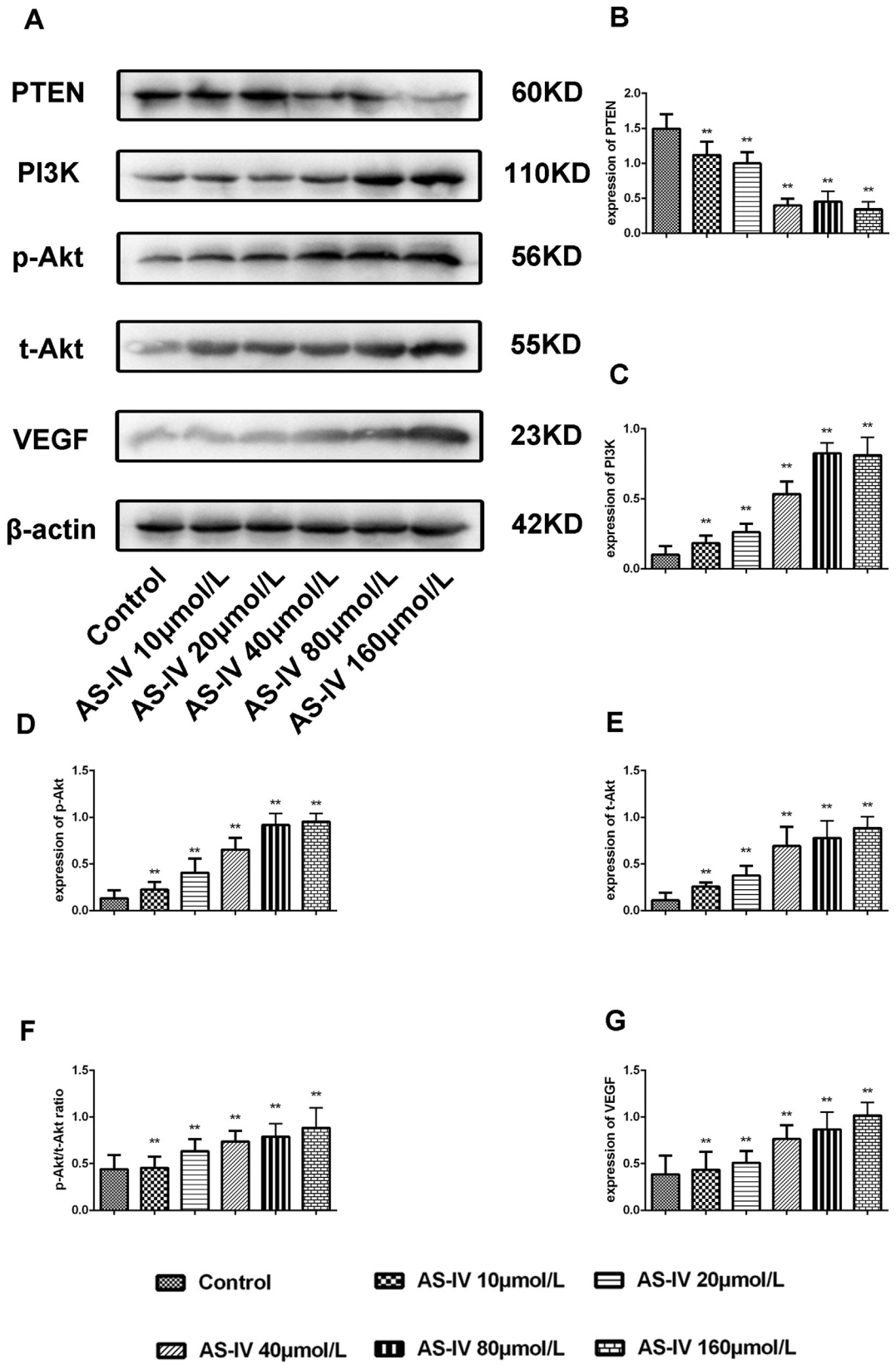

Fig. 8. Assessment of signaling pathway activation after treatment in vitro. (A) Expression of PTEN/PI3K/Akt signaling pathway and VEGF from HUVECs cultivated with different dosage of AS-IV. Quantified western blot results of PTEN(B), PI3K (C), p-Akt (D), t-Akt(E), p-Akt/p-Akt ratio (F) and VEGF (G)are provided.β-actin served as the internal control.**P $<$ 0.01 compared with the control group. AS-IV, astragaloside IV.

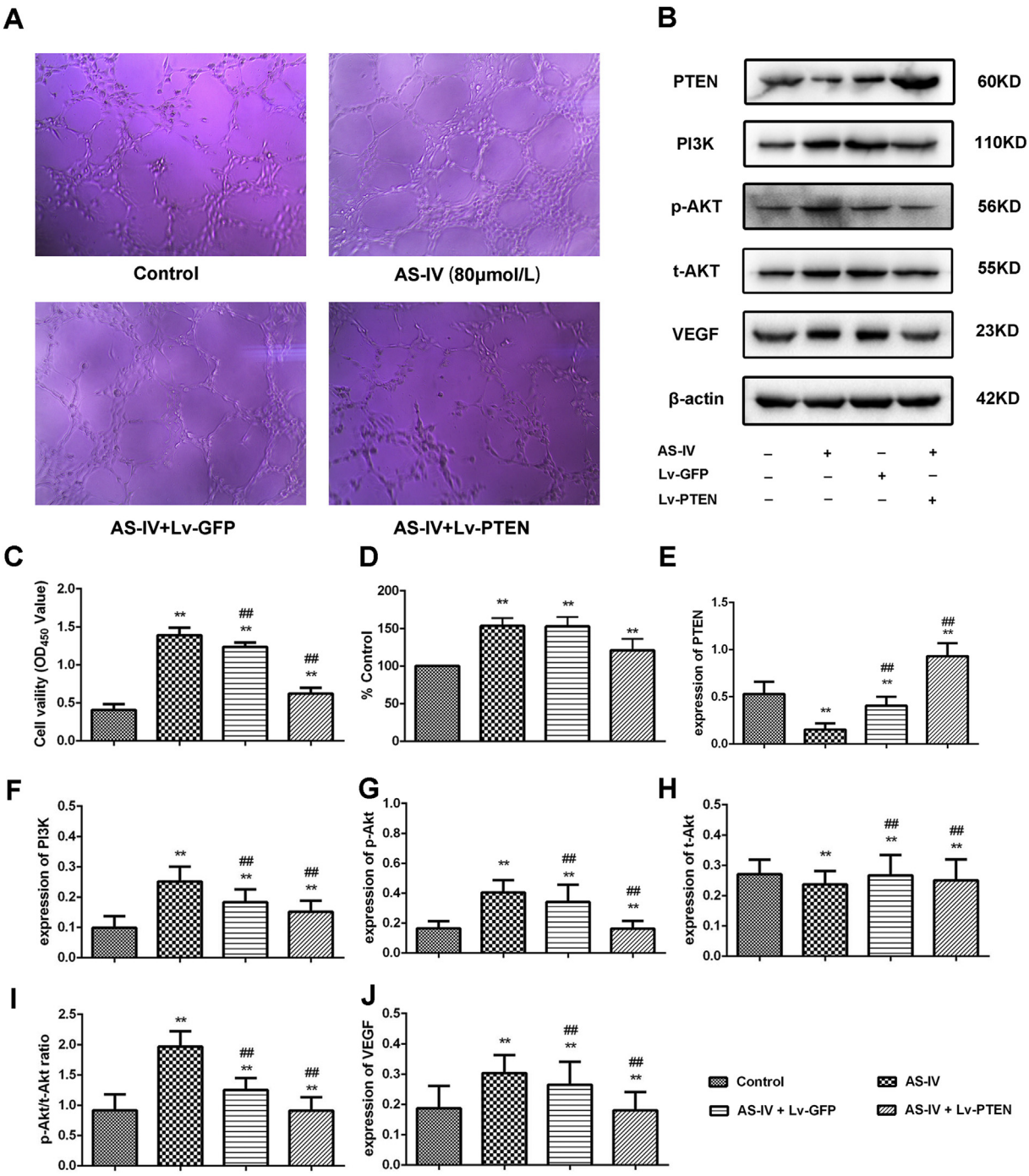

Fig. 9. (A) Representative images of Matrigel tube formation assay analysis at 200× magnification. HUVECs were treated with different conditions. (B) Expression of PTEN/PI3K/Akt signaling pathway and VEGF from HUVECs cultivated with different conditions. (C) Proliferation of HUVECs treated with different conditions was detected by CCK-8 assay. (D) Bar graph of tube formation assessment with different conditions, data were analyzed as tube percentage versus control group. Quantified western blot results of PTEN(E), PI3K (F), p-Akt (G), t-Akt(H), p-Akt/p-Akt ratio (I) and VEGF (J)are provided.β-actin served as the internal control.**P < 0.01 compared with the control group. ##P < 0.01 compared with the AS-IV group. AS-IV, astragaloside IV; CCK-8, Cell Counting kit 8; Lv, lentivirus.

Akt was also observed in vivo. In vitro research indicated that AS-IV was able to enhance cell proliferation and tube formation in HUVECs. Furthermore, PTEN/PI3K/Akt signaling pathway was identified that took a critical part in AS-IV induced angiogenesis.

Angiogenesis is a complex process that has the potential to rescue myocardial at early stages after AMI, it's crucial for preventing subsequent ischemic-related heart failure as well [20]. Several factors trigger angiogenesis such as hypoxia [21], inflammation [22], progenitor cells [23] and growth factors [24]. Up to date, the most popular approach to stimulate angiogenesis after AMI is to deliver progenitor cells or growth factors. Nevertheless, several studies failed to indicate any potential benefit on left ventricular systolic or diastolic function. Some methodological controversies, such as way of delivery for growth factors or progenitor cells might partially explain the failure of such trials [25]. An increasing number of extraction from natural productions are reported as potent stimulus of neovascularization [26–28]. In the present study, extraction of Astragalus membranaceus with high bioactivity was investigated to figure out the putative pro-angiogenesis

mechanism.

Phosphatase and tensin homolog deleted on chromosome ten (PTEN) was initially found as a tumor suppressor in several human cancers such as endometrial cancer [29], prostate cancer [30] and small cell lung cancer [31], it dephosphorylates phosphatidylinositol (3,4,5)-triphosphate (PIP3), therefore represses the activation of phosphatidylinositol-3-kinase (PI3K)/Akt signaling pathway. Furthermore, regulation of PTEN affects the pathogenesis not only in cancer, but also other diseases [32], however, high expression of PTEN might results in several pathological processes as well. Inhibition of PTEN showed neuroprotective effect in mouse models of Parkinson's disease [33]. Overexpression of PTEN contributed to thrombosis formation by inducing endothelial dysfunction [34]. It was reported that downregulation of PTEN could promote angiogenesis through increasing the expression of VEGF, together with reinforcing the signal transduction of VEGF-bind cells [35,36]. All those above indicated that regulating PTEN related signaling pathway has potential of promoting angiogenesis after AMI. Our present study has provided an alternative way to activate angiogenesis associated signaling pathway by natural herbal extract.

To figure out the mechanisms by which AS-IV administration triggered PTEN/PI3K/Akt signaling pathway, we performed in vitro study using lentivirus transfection and found that AS-IV administration downregulated the expression of PTEN and enhanced angiogenesis, whereas increased the level of PTEN by lentivirus transfection resulted in inhibition of angiogenesis induced by AS-IV. However, one limitation is that we did not carry out in vivo experiment to support our thesis. Despite the limitation, our data confirmed that angiogenesis and cardioprotective effects induced by AS-IV are mediated through a PTEN/PI3K/Akt-dependent mechanism.

5. Conclusion

In summary, our study demonstrates that Astragaloside IV protects cardiac function against AMI by enhancing angiogenesis. This cardioprotective effect is associated with PTEN/PI3K/Akt-dependent mechanism. These findings advance our understanding of the underlying mechanisms in angiogenesis after AMI, and suggest Chinese herbal extracts as novel therapeutic agents.

Conflict of interest policy form and author contribution to study form

S. C., L. Y., H. Z., X.Z. and L. S. performed in vivo experiments, S. C., Q. F. and P. Y. performed in vitro experiments, J. C., W. S. and D. C. analyzed data, S. C. drafted the manuscript. X. C. contributed in experimental design. All authors approve final version of manuscript and declare that there is no conflict of interest.

Acknowledgements

This study was granted by National Natural Science Foundation of China (no. 81573908), Jiangsu Province Natural Science Foundation (no. BK20171099) and Project Funded by Jiangsu Provincial Administration of Traditional Chinese Medicine (no. ZD201703).

Disclosures

There is no conflict of interest.

References

[1] K. Thygesen, J.S. Alpert, A.S. Jaffe, B.R. Chaitman, J.J. Bax, D.A. Morrow, H.D. White, Fourth universal definition of myocardial infarction (2018), Eur. Heart J. 40 (3) (2018) 237–269.
[2] L. Saaby, T.S. Poulsen, S. Hosbond, T.B. Larsen, A.C. Pyndt Diederichsen, J. Hallas, K. Thygesen, H. Mickley, Classification of myocardial infarction: frequency and features of type 2 myocardial infarction, Am. J. Med. 126 (9) (2013) 789–797.
[3] F. Alfonso, F. Rivero, Value of different physiological indexes to defer coronary revascularization, JACC Cardiovasc. Interv. 11 (15) (2018) 1450–1453.
[4] F. Yuan, L. Guo, K.H. Park, J.R. Woollard, K. Taek-Geun, K. Jiang, T. Melkamu, B. Zang, S.L. Smith, S.C. Fahrenkrug, F.D. Kolodgie, A. Lerman, R. Virmani, L.O. Lerman, D.F. Carlson, Ossabaw pigs with a PCSK9 gain-of-function mutation develop accelerated coronary atherosclerotic lesions: a novel model for preclinical studies, J. Am. Heart Assoc. 7 (6) (2018) (pii: e006207).
[5] H. Okura, S. Nezuo, K. Yoshida, Successful stent implantation guided by intravascular ultrasound and a Doppler guidewire without contrast injection in a patient with allergy to iodinated contrast media, J. Invasive Cardiol. 23 (7) (2011) 297–299.
[6] P. Carmeliet, R.K. Jain, Molecular mechanisms and clinical applications of angiogenesis, Nature 473 (7347) (2011) 298–307.
[7] D.W. Losordo, S. Dimmeler, Therapeutic angiogenesis and vasculogenesis for ischemic disease: part II: cell-based therapies, Circulation 109 (22) (2004) 2692–2697.
[8] N. Ferrara, H.P. Gerber, J. LeCouter, The biology of VEGF and its receptors, Nat. Med. 9 (6) (2003) 669–676.
[9] M. Murakami, M. Simons, Fibroblast growth factor regulation of neovascularization, Curr. Opin. Hematol. 15 (3) (2008) 215–220.
[10] J. Tongers, D.W. Losordo, U. Landmesser, Stem and progenitor cell-based therapy in ischaemic heart disease: promise, uncertainties, and challenges, Eur. Heart J. 32 (10) (2011) 1197–1206.
[11] S. Ren, H. Zhang, Y. Mu, M. Sun, P. Liu, Pharmacological effects of Astragaloside IV: a literature review, J. Tradit. Chin. Med. 33 (3) (2013) 413–416.
[12] W.N. Yu, L.F. Sun, H. Yang, Inhibitory effects of astragaloside IV on bleomycin-induced pulmonary fibrosis in rats via attenuation of oxidative stress and inflammation, Inflammation 39 (5) (2016) 1835–1841.
[13] T. Chen, R. Wang, W. Jiang, H. Wang, A. Xu, G. Lu, Y. Ren, Y. Xu, Y. Song, S. Yong, H. Ji, Z. Ma, Protective effect of astragaloside IV against paraquat-induced lung injury in mice by suppressing Rho signaling, Inflammation 39 (1) (2016) 483–492.
[14] D. Gui, J. Huang, W. Liu, Y. Guo, W. Xiao, N. Wang, Astragaloside IV prevents acute kidney injury in two rodent models by inhibiting oxidative stress and apoptosis pathways, Apoptosis 18 (4) (2013) 409–422.
[15] S. Zhang, F. Tang, Y. Yang, M. Lu, A. Luan, J. Zhang, J. Yang, H. Wang, Astragaloside IV protects against isoproterenol-induced cardiac hypertrophy by regulating NF-kappaB/PGC-1alpha signaling mediated energy biosynthesis, PLoS One 10 (3) (2015) e0118759.
[16] L. Tu, C.S. Pan, X.H. Wei, L. Yan, Y.Y. Liu, J.Y. Fan, H.N. Mu, Q. Li, L. Li, Y. Zhang, K. He, X.W. Mao, K. Sun, C.S. Wang, C.C. Yin, J.Y. Han, Astragaloside IV protects heart from ischemia and reperfusion injury via energy regulation mechanisms, Microcirculation 20 (8) (2013) 736–747.
[17] B. Leng, F. Tang, M. Lu, Z. Zhang, H. Wang, Y. Zhang, Astragaloside IV improves vascular endothelial dysfunction by inhibiting the TLR4/NF-kappaB signaling pathway, Life Sci. 209 (2018) 111–121.
[18] D.Q. Zhang, J.S. Li, Y.M. Zhang, F. Gao, R.Z. Dai, Astragaloside IV inhibits angiotensin II-stimulated proliferation of rat vascular smooth muscle cells via the regulation of CDK2 activity, Life Sci. 200 (2018) 105–109.
[19] S.G. Wang, Y. Xu, J.D. Chen, C.H. Yang, X.H. Chen, Astragaloside IV stimulates angiogenesis and increases nitric oxide accumulation via JAK2/STAT3 and ERK1/2 pathway, Molecules 18 (10) (2013) 12809–12819.
[20] C. Cochain, K.M. Channon, J.S. Silvestre, Angiogenesis in the infarcted myocardium, Antioxid. Redox Signal. 18 (9) (2013) 1100–1113.
[21] C.W. Pugh, P.J. Ratcliffe, Regulation of angiogenesis by hypoxia: role of the HIF system, Nat. Med. 9 (6) (2003) 677–684.
[22] N.G. Frangogiannis, C.W. Smith, M.L. Entman, The inflammatory response in myocardial infarction, Cardiovasc. Res. 53 (1) (2002) 31–47.
[23] G.P. Fadini, D. Losordo, S. Dimmeler, Critical reevaluation of endothelial progenitor cell phenotypes for therapeutic and diagnostic use, Circ. Res. 110 (4) (2012) 624–637.
[24] S. Miyagawa, Y. Sawa, S. Taketani, N. Kawaguchi, T. Nakamura, N. Matsuura, H. Matsuda, Myocardial regeneration therapy for heart failure: hepatocyte growth factor enhances the effect of cellular cardiomyoplasty, Circulation 105 (21) (2002) 2556–2561.
[25] H. Haider, S.A. Akbar, M. Ashraf, Angiomyogenesis for myocardial repair, Antioxid. Redox Signal. 11 (8) (2009) 1929–1944.
[26] P. Shi, Y. Cao, J. Gao, B. Fu, J. Ren, L. Ba, C. Song, H. Qi, W. Huang, X. Guan, H. Sun, Allicin improves the function of cardiac microvascular endothelial cells by increasing PECAM-1 in rats with cardiac hypertrophy, Phytomedicine 51 (2018) 241–254.
[27] L.J. Yu, K.J. Zhang, J.Z. Zhu, Q. Zheng, X.Y. Bao, S. Thapa, Y. Wang, Salvianolic acid exerts cardioprotection through promoting angiogenesis in animal models of acute myocardial infarction: preclinical evidence, Oxidative Med. Cell. Longev. 2017 (2017) 8192383.
[28] B.R. Yang, K.K. Cheung, X. Zhou, R.F. Xie, P.P. Cheng, S. Wu, Z.Y. Zhou, J.Y. Tang, P.M. Hoi, Y.H. Wang, S.M. Lee, Amelioration of acute myocardial infarction by saponins from flower buds of Panax notoginseng via pro-angiogenesis and anti-apoptosis, J. Ethnopharmacol. 181 (2016) 50–58.
[29] M.D. Forster, K.J. Dedes, S. Sandhu, S. Frentzas, R. Kristeleit, A. Ashworth, C.J. Poole, B. Weigelt, S.B. Kaye, L.R. Molife, Treatment with olaparib in a patient with PTEN-deficient endometrioid endometrial cancer, Nat. Rev. Clin. Oncol. 8 (5) (2011) 302–306.
[30] P. Cairns, K. Okami, S. Halachmi, N. Halachmi, M. Esteller, J.G. Herman, J. Jen, W.B. Isaacs, G.S. Bova, D. Sidransky, Frequent inactivation of PTEN/MMAC1 in primary prostate cancer, Cancer Res. 57 (22) (1997) 4997–5000.
[31] J.C. Soria, H.Y. Lee, J.I. Lee, L. Wang, J.P. Issa, B.L. Kemp, D.D. Liu, J.M. Kurie,

L. Mao, F.R. Khuri, Lack of PTEN expression in non-small cell lung cancer could be related to promoter methylation, Clin. Cancer Res. 8 (5) (2002) 1178–1184.
[32] W. Li, T. Zhang, L. Guo, L. Huang, Regulation of PTEN expression by noncoding RNAs, J. Exp. Clin. Cancer Res. 37 (1) (2018) 223.
[33] A. Domanskyi, C. Geissler, I.A. Vinnikov, H. Alter, A. Schober, M.A. Vogt, P. Gass, R. Parlato, G. Schutz, Pten ablation in adult dopaminergic neurons is neuroprotective in Parkinson's disease models, FASEB J. 25 (9) (2011) 2898–2910.
[34] H.M. Kuo, C.Y. Lin, H.C. Lam, P.R. Lin, H.H. Chan, J.C. Tseng, C.K. Sun, T.F. Hsu, C.C. Wu, C.Y. Yang, C.M. Hsu, M.H. Tai, PTEN overexpression attenuates angiogenic processes of endothelial cells by blockade of endothelin-1/endothelin B receptor signaling, Atherosclerosis 221 (2) (2012) 341–349.
[35] B.H. Jiang, J.Z. Zheng, M. Aoki, P.K. Vogt, Phosphatidylinositol 3-kinase signaling mediates angiogenesis and expression of vascular endothelial growth factor in endothelial cells, Proc. Natl. Acad. Sci. U. S. A. 97 (4) (2000) 1749–1753.
[36] H.D. Skinner, J.Z. Zheng, J. Fang, F. Agani, B.H. Jiang, Vascular endothelial growth factor transcriptional activation is mediated by hypoxia-inducible factor 1alpha, HDM2, and p70S6K1 in response to phosphatidylinositol 3-kinase/AKT signaling, J. Biol. Chem. 279 (44) (2004) 45643–45651.